The Astrophysical Journal Letters, 878:L11 (4pp), 2019 June 10 https://doi.org/10.3847/2041-8213/ab238e

The Star Formation History in the Solar Neighborhood as Told by Massive White Dwarfs

Jordi Isern[1,2]
[1] Institut de Ciències de l'Espai (ICE, CSIC), C/Can Magrans, Campus UAB, E-08193 Cerdanyola, Spain; isern@ice.cat, isern@ieec.cat
[2] Institut d'Estudis Espacials de Catalunya (IEEC), Ed. Nexus-201, c/Gran Capità 2-4, E-08034 Barcelona, Spain
Received 2019 April 27; revised 2019 May 21; accepted 2019 May 22; published 2019 June 6

Abstract

White dwarfs (WDs) are the remnants of low- and intermediate-mass stars. Because of electron degeneracy, their evolution is just a simple gravothermal process of cooling. Recently, thanks to *Gaia* data, it has been possible to construct the luminosity function of massive ($0.9 \leqslant M/M_{\odot} \leqslant 1.1$) WDs in the solar neighborhood ($d < 100$ pc). Because the lifetime of their progenitors is very short, the birth times of both parents and daughters are very close and facilitate the reconstruction of an (effective) star formation rate. This rate started growing from zero during the early Galaxy and reached a maximum 6–7 Gyr ago. It declined and ∼5 Gyr ago started to climb once more, reaching a maximum 2–3 Gyr ago; it has decreased since then. There are some traces of a recent star formation burst, but the method used here is not appropriate for recently born WDs.

Key words: Galaxy: evolution – solar neighborhood – white dwarfs

1. Introduction

The luminosity function is defined as the number of white dwarfs (WDs) of a given luminosity per unit volume (or galactic disk surface unit, for instance) and magnitude interval (hereafter WDLF):

$$N(l) = \int_{M_{\rm i}}^{M_{\rm s}} \Phi(M)\Psi[T - t_{\rm cool}(l, M) - t_{\rm PS}(M)]\tau_{\rm cool}(l, M)\, dM \quad (1)$$

where T is the age of the population under study, $l = -\log(L/L_{\odot})$, M is the mass of the parent star (for convenience all WDs are labeled with the mass of the main-sequence progenitor), $t_{\rm cool}$ is the cooling time down to luminosity l, $\tau_{\rm cool} = dt/dM_{\rm bol}$ is the characteristic cooling time, $M_{\rm s}$ is the maximum mass of a main-sequence star able to produce a WD, and $M_{\rm i}$ is the minimum mass of the main-sequence stars able to produce a WD of luminosity l, i.e., the mass that satisfies the condition $T = t_{\rm cool}(l, M) + t_{\rm PS}(M)$, and $t_{\rm PS}$ is the lifetime of the progenitor star. The remaining quantities, the initial mass function (IMF), $\Phi(M)$, and the star formation rate (SFR), $\Psi(t)$, are not known a priori and depend on the astronomical properties of the stellar population under study. As the total density of WDs of a given population is usually not well known, it is customary to normalize the computed luminosity function to a bin with a small error bar in order to compare theoretical and observational data. For instance, in the case of the disk this bin is usually $l = 3$. Therefore, if the observed luminosity function and the evolutionary behavior of WDs are known, it is possible to obtain information about the properties of the population under study. Evidently, given the nature of the problem, there is always a degeneracy between the galactic properties (SFR and IMF) and the adopted stellar models.

The process of obtaining such information can be formulated as follows. Let $t_b = T_{\rm disk} - t_{\rm cool}(l, M) - t_{\rm PS}(M)$ be the time at which the progenitor of the WD was born, and $M = M(t_b)$ be the mass of the star that being born at this time is able to produce a WD of luminosity l at present. Equation (1) can be written as

$$N(l) = \int_0^{t_b^{up}} K(l, t_b)\Psi(t_b)dt_b \quad (2)$$

with

$$K(l, t_b) = \Phi[M(t_b)]\tau_{\rm cool}[l, M(t_b)]\frac{dM(t_b)}{dt_b}. \quad (3)$$

The kernel, $K(l, t_b)$, of this integral function is not symmetric in l and t_b and it behaves in quite a complicated manner. Consequently, according the Picard–Lindelöf's theorem, Ψ cannot be directly obtained and the uniqueness of the solution is not guaranteed (Isern et al. 1995).

One way to tackle this problem is to optimize the parameters of some trial functions comparing, after defining some weight function, models with data (Isern et al. 1999). Obviously, this solution is optimal within the context of the adopted model, which might not correspond with the reality. Another way consists of starting from a simple initial estimate of the SFR, and iteratively improving the solution using all the observational bins until a satisfactory solution is found (Rowell 2013a). This solution is quite sensitive to the adopted metallicity and IMF, but not to the DA (hydrogen-rich) or non-DA (hydrogen-poor) WD ratio, and also not to the relationship between the mass of the WD and that of the progenitor. All in all, the quality of the final solution essentially depends on the quality of the observational data.

Finally, if the luminosity function is restricted to massive WDs, then the SFR can be directly obtained (Diaz-Pinto et al. 1994). This method, however, has suffered from the scarcity of known high-mass WDs. In an early work, this SFR was obtained from the data of Sion et al. (1988) and Bergeron et al. (1992), and also from Leggett et al. (1998), but the relatively small number of stars in the sample prevented any firm conclusions (Isern et al. 1999). Fortunately this situation has recently changed thanks to the work of Tremblay et al. (2019) who have been able to build a reliable and precise luminosity function of massive stars using the data provided by *Gaia*.

2. Massive WDs and the SFR

This luminosity function, averaged over an interval of luminosity Δl, can also be directly computed as follows (Isern et al. 1999). Assume a stellar population that forms at a rate $\Psi(t)$. After a time T, the number of WDs that have a luminosity l per unit of luminosity interval is given by

$$N(l, T) = \frac{1}{\Delta l}\int_t\int_M \Phi(M)\Psi(t)dMdt \quad (4)$$

where, as before, M is the mass of the parent star, and the integral is constrained to the domain

$$T - t_{\rm cool}(M, l - 0.5\Delta l) \leqslant t + t_{\rm MS}(M) \leqslant T - t_{\rm cool}(M, l + 0.5\Delta l) \quad (5)$$

for all of the stars that are able to produce a WD.

If the integral is restricted to massive WDs, i.e., those for which it is possible to neglect the lifetime of the progenitor in front of the cooling time, and $\Psi(t)$ is smooth enough,[3] then

$$N(l, T) \simeq \frac{\langle\Psi\rangle}{\Delta l}\int_{\Delta M} \Phi(M)\Delta t_{\rm cool}(l, M)dM \quad (6)$$

with

$$\Delta t_{\rm cool} = t_{\rm cool}(l + 0.5\Delta l, M) - t_{\rm cool}(l - 0.5\Delta l, M) \quad (7)$$

and consequently,

$$\langle\Psi\rangle = \frac{N(l, T)\Delta l}{\int_{\Delta M}\Phi(M)\Delta t_{\rm cool}(l, M)dM} \quad (8)$$

$$\langle t\rangle = \frac{\int_{\Delta M}\Phi(M)tdM}{\int_{\Delta M}\Phi(M)dM} \quad (9)$$

$$\langle\Delta t\rangle = \frac{\int_{\Delta M}\Phi(M)\Delta tdM}{\int_{\Delta M}\Phi(M)dM}. \quad (10)$$

It is important to notice here that the SFR obtained in this way is effective in the sense that it recovers the present age distribution of the sample, but does not take into account the secular evolution of the sample mainly due to radial migrations and height inflation. On another hand, hidden WDs in binaries and non-resolved double degenerates can bias the sample. In addition, double-degenerate mergers can reduce the density of WDs in some bins; in the case that they do not explode as Type Ia supernovae, they reappear as newly born hot single WDs with the corresponding density increase of younger bins, thus modifying the SFR deduced from these data. The importance of this effect is small given the present level of precision, but it will be necessary to include it in order to interpret future high-precision WDLFs.

3. Results and Conclusions

Table 1 shows the values taken by $\langle\Psi\rangle$, $\langle t\rangle$, and $\langle\Delta t\rangle$ using the Tremblay et al. (2019) data and the BaSTI models[4] for DA WDs. Models labeled *ns* take into account only the release of latent heat upon crystallization, while models labeled *s* also take into account the gravitational energy released by the sedimentation induced by the changes of solubility during the crystallization process. Both families of models are built with the chemical profiles predicted by the evolution of the progenitor that depends on the mass (Salaris et al. 2019). The relationship between the masses of the progenitor and WD is that found by El-Badry et al. (2018),[5] while the IMF is that of Salpeter truncated at 0.1 $M_\odot$ and normalized to the unit mass.

Figure 1 displays these results, where blue and black dots correspond to the calculations with and without sedimentation,

Table 1
Total SFR Ψ ($M_\odot$ Gyr^{-1} pc^{-3}), Age, t and Time Interval Δt (Gyr) Obtained from each Luminosity Function Bin

$\log_{10}(L/L_\odot)$	t_s	Δt_s	$\log_{10}\Psi_s$	t_{ns}	$\Delta\ t_{ns}$	$\log_{10}\Psi_{ns}$
−1.20	0.05	0.04	−2.794	0.05	0.04	−2.794
−1.70	0.12	0.16	−2.553	0.12	0.16	−2.553
−2.30	0.41	0.43	−2.655	0.41	0.42	−2.643
−2.80	0.97	0.81	−2.780	0.91	0.64	−2.678
−3.10	1.80	0.70	−2.546	1.53	0.52	−2.418
−3.30	2.59	0.88	−2.468	2.13	0.67	−2.350
−3.50	3.53	0.99	−2.600	2.86	0.80	−2.508
−3.70	4.58	1.11	−2.747	3.75	0.98	−2.694
−3.90	5.75	1.23	−2.753	4.82	1.16	−2.728
−4.10	7.06	1.46	−2.667	6.09	1.43	−2.660
−4.30	8.88	2.58	−2.885	7.89	2.57	−2.884
−4.50	11.95	2.82	−3.403	10.96	2.82	−3.403
−4.70	14.13	1.66	−4.123	13.14	1.68	−4.130

Note. Sub-indexes *s* and *ns* correspond to the cases with and without sedimentation.

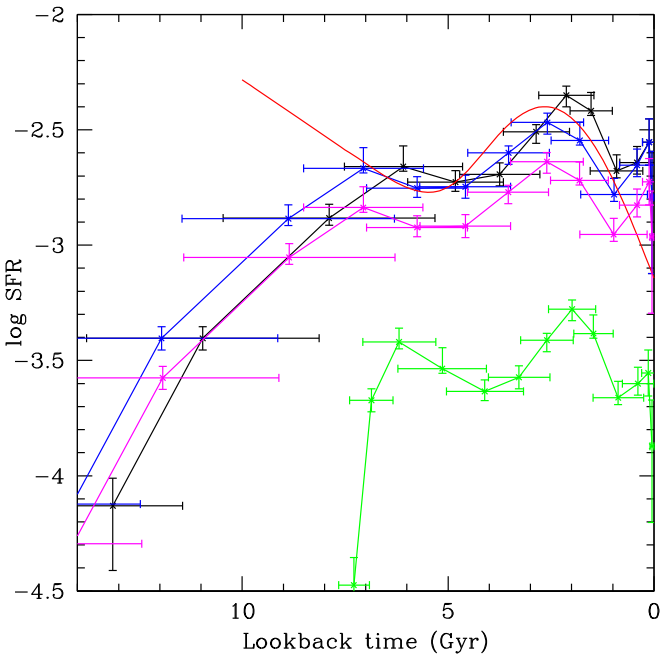

Figure 1. SFR ($M_\odot$ Gyr^{-1} pc^{-3}) in the solar neighborhood obtained from massive WDs ($d \leqslant 100$ pc). Blue dots were computed taking into account the energy released by crystallization (latent heat) and induced sedimentation, and black ones only latent heat. The red line represents the SFR per unit of disk surface obtained from main-sequence stars (Mor et al. 2019), divided by the arbitrary scale height to allow for comparison. Magenta points were computed in the same way as the blue ones but using the IMF of Mor et al. (2019). Green points represent the SFR, divided by 10 for clarity, obtained using the Montreal models.

[3] This method is also valid for WDs with masses within a limited range of values.
[4] Cooling models publically available at http://albione.oa-teramo.inaf.it.
[5] The results obtained with the Catalán et al. (2008) initial-final mass relationship are similar.

respectively. As can be seen, in both cases the effective SFR is not a monotonically decreasing or constant function as it is often assumed. It grew quickly in the past, during the first epochs of the Galaxy, roughly stabilized, and then started to decrease 7 or 6 Gyr ago (cases *s* and *ns*, respectively) around the values $\log_{10}\Psi \approx -2.4, -2.8\ M_{\odot}\,\mathrm{Gyr}^{-1}\,\mathrm{pc}^{-3}$. A noticeable feature is the prominent peak centered at 2.8 or 2.2 Gyr ago depending on the adopted cooling model. The increase of the SFR near the present time is not reliable because it does not satisfy the hypothesis of a negligible main-sequence lifetime versus cooling time; this deserves more attention.

A hint of this behavior, a bump centered around 2–3 Gyr, was already present in the results obtained by Isern et al. (1999) —see their Figure 2—but it was not interpreted as indicative of star formation variability. The small number of stars in the sample prevented its identification, in contrast with the present situation where the quality of the Tremblay et al. (2019) luminosity function provides a robust argument in favor of the non-monotonous behavior of the SFR.

Interestingly, Rowell (2013a, 2013b) inverted the total luminosity functions obtained by Harris et al. (2006) and Rowell & Hambly (2011) from the Sloan and the Super-COSMOS Sky Surveys, respectively, and found in both cases a solution characterized by two peaks of star formation, placed at ∼9 and 2–3 Gyr in the past; this is in qualitative agreement with the results found here.

The existing degeneracy between galactic properties and evolutionary models implies that different models can lead to different star formation histories. The green dots of Figure 1 display the evolution of the SFR obtained with the Monreal models[6] COXXX0210, which are made of a half-oxygen, half-carbon core, an He-layer of $10^{-2}\ M_{\odot}$, and an H-layer of $10^{-10}\ M_{\odot}$; this does not take into account sedimentation. In this case the bump is present, but the star formation abruptly starts around ∼7 Gyr.

One way to remove this degeneracy is to compare these results with other star formation histories that have been obtained with independent methods. The red line of Figure 1 displays, after dividing by an arbitrary scale height to facilitate comparison, the SFR per unit of galactic surface disk obtained with the *Gaia* second data release (DR2) for main-sequence stars with $G \leqslant 12$ in the context of the Besançon Galaxy Model (Mor et al. 2019). This analysis suggests a decreasing trend in the interval of 9–10 to 6–7 Gyr followed by a starburst with a maximum centered at 2–3 Gyr. Magenta dots were obtained as in the sedimentation case but adopting the IMF proposed by Mor et al. (2019) in their analysis of the *Gaia* data. The similarity of both computed SFRs is due to the fact that this IMF is not too different from the Salpeter one in the region corresponding to the masses of the progenitors of the massive WDs considered here. Two factors deserve attention. (i) The position and the width of the SFR burst obtained by Mor et al. (2019) seems to favor models including sedimentation, and (ii) the local and the disk SFR seem to diverge at the early epochs of the Galaxy. The second factor has several potential origins, and demands further attention. One possibility is a delay in the beginning of the star formation process with respect to inner regions of the disk (Kubryk et al. 2015), or perhaps the outer disk behaves differently compared with the inner one, as proposed by Haywood et al. (2018). Another possibility is a vertical dilution induced by a galactic collision like the *Gaia*-Enceladus event (Helmi et al. 2018).

[6] http://www.astro.umontreal.ca/~bergeron/CoolingModels

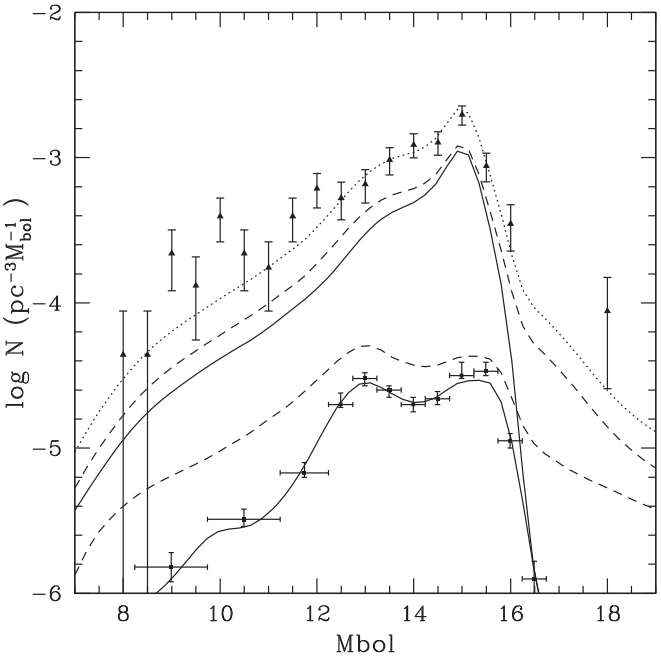

Figure 2. Theoretical luminosity functions obtained from the SFR of Table 1 (case *s*). Solid lines: massive (bottom) and all masses (top) DAs, excepting ONe ones. Dashed lines: all massive WDs (DAs and non-DAs and ONe ones (bottom) and all DAs (top). Dotted line: the same as the top dashed line, but normalized to the total luminosity function. Squares: DA WDs of all masses excepting ONe ones Tremblay et al. (2019). Triangles: all WDs (Oswalt et al. 2017).

As the SFR has been derived from the tail of the mass distribution of WDs and neglecting the lifetime of the progenitor, it is natural to check if it can reproduce the luminosity function of all WDs in the solar vicinity. For that purpose, Figure 2 displays a luminosity function that is representative of all WDs present in a volume of 25 pc around the Sun; it is believed to be 68% complete (Oswalt et al. 2017). Figure 2 also displays the luminosity function of massive DA white dwarfs and the corresponding theoretical counterpart (solid line). The dashed line is obtained when non-DAs and WDs with massive ONe cores are included. The total luminosity function is represented by black lines (dashed for all WDs, and solid for DAs with CO cores only). As can be seen, the shape is well reproduced except for a peak at $M_{\rm bol} \sim 9$, which can be accounted for by placing a burst at ∼0.4 Gyr; this is within the limit of the method presented in this Letter. A potential problem is that the total WDLF predicted with the SFR obtained here is a factor ∼3 smaller than the observed one.

The uncertainties in the IMF and in the initial-final mass relationship, as well as the way that the scale height over the galactic plane is included, alleviates the discrepancy but does not solve it. Other possibilities are the degree of completeness of the solar sample or the secular galactic evolution in the solar neighborhood, but given the present uncertainties it is not possible to obtain any definite conclusion and it will be necessary to wait for a distribution not only in luminosities, but also in masses obtained from the same sample with the same method for all of them.

In conclusion, massive WDs provide a robust argument in favor of a star formation burst in the solar neighborhood that

occurred 2–3 Gyr ago, as well as a hint of the existence of a more recent one, around 0.4–0.3 Gyr. These results are a clear demonstration of the possibilities offered by WD cosmochronology for studying the evolution of the Galaxy and the need to completely understand their physical properties.

This work has been supported by MINECO grant ESP2017-82674-R, EU FEDER funds, grant 2014SGR1458, and the CERCA Programme of the Generalitat de Catalunya.

ORCID iDs

Jordi Isern https://orcid.org/0000-0002-0819-9574

References

Bergeron, P., Saffer, R. A., & Liebert, J. 1992, ApJ, 394, 228
Catalán, S., Isern, J., García-Berro, E., & Ribas, I. 2008, MNRAS, 387, 1693
Diaz-Pinto, A., García-Berro, E., Hernanz, M., Isern, J., & Mochkovitch, R. 1994, A&A, 282, 86
El-Badry, K., Rix, H.-W., & Weisz, D. R. 2018, ApJL, 860, L17
Harris, H. C., Munn, J. C., Kilic, M., et al. 2006, AJ, 131, 571
Haywood, M., Di Matteo, P., Lehnert, M., et al. 2018, A&A, 618, A78
Helmi, A., Babusiaux, C., Koppelman, H. H., et al. 2018, Natur, 563, 85
Isern, J., García-Berro, E., Hernanz, M., et al. 1995, LNP, 443, 19
Isern, J., Hernanz, M., García-Berro, E., & Mochkovitch, R. 1999, in ASP Conf. Ser. 169, 11th European Workshop on White Dwarfs, ed. S. E. Solheim & E. G. Meistas (San Francisco, CA: ASP), 408
Kubryk, M., Prantzos, N., & Athanassoula, E. 2015, A&A, 580, A126
Leggett, S. K., Ruiz, M. T., & Bergeron, P. 1998, ApJ, 497, 294
Mor, R., Robin, A. C., Figueras, F., Roca-Fàbrega, S., & Luri, X. 2019, arXiv:1901.07564
Oswalt, T. D., Holberg, J., & Sion, E. 2017, in ASP Conf. Ser. 509, 20th European White Dwarf Workshop, ed. P. E. Tremblay et al. (San Francisco, CA: ASP), 59
Rowell, N. 2013a, MNRAS, 434, 1549
Rowell, N. 2013b, in ASP Conf. Ser. 469, 18th European White Dwarf Workshop, ed. J. Krzesinsky et al. (San Francisco, CA: ASP), 89
Rowell, N., & Hambly, N. C. 2011, MNRAS, 417, 93
Salaris, M., Cassisi, S., Pietrinferni, A., Kowalski, P. M., & Isern, J. 2019, ApJ, 716, 1241
Sion, E. M., Fritz, M. L., McMullin, J. P., & Lallo, M. D. 1988, AJ, 96, 251
Tremblay, P.-E., Fontaine, G., Fusillo, N. P. G., et al. 2019, Natur, 565, 202